Cell Mol Neurobiol (2008) 28:371–388
DOI 10.1007/s10571-007-9253-y

ORIGINAL PAPER

Spatiotemporal Expression of Dexras1 After Spinal Cord Transection in Rats

Xin Li · Chun Cheng · Min Fei · Shangfeng Gao · Shuqiong Niu · Mengling Chen · Yonghua Liu · Zhiqin Guo · Haibo Wang · Jian Zhao · Xiaowei Yu · Aiguo Shen

Received: 27 September 2007 / Accepted: 11 December 2007 / Published online: 25 January 2008

Abstract Dexras1, a brain-enriched member of the Ras subfamily of GTPases, as a novel physiologic nitric oxide (NO) effector, anchor neuronal nitric oxide synthase (nNOS) that increased after spinal cord injury (SCI), to specific targets to enhance NO signaling, and is strongly and rapidly induced during treatment with dexamethasone. It is unknown how the central nervous system (CNS) trauma affects the expression of Dexras1. Here we used spinal cord transection (SCT) model to detect expression of Dexras1 at mRNA and protein level in spinal cord homogenates by real-time PCR and Western blot analysis. The results showed that Dexras1 mRNA upregulated at 3 day, 5 day, and 7 day significantly ($P < 0.05$) that was consistent with the protein level except at 7 day. Immunofluorescence revealed that both neurons and glial cells showed Dexras1 immunoreactivivty (IR) around SCT site, but the proportion is different. Importantly, injury-induced expression of Dexras1 was co-labeled by caspase-3 (apoptotic marker) and Tau-1 (marker for pathological oligodendrocyte).

Xin Li, Chun Cheng, and Min Fei contributed equally to this work.

X. Li · S. Niu · Z. Guo · A. Shen (✉)
The Jiangsu Province Key Laboratory of Neuroregeneration, Nantong University, 19 Qi-xiu Road, Nantong, Jiangsu 226001, China
e-mail: Shen_aiguo@yahoo.com

X. Li · C. Cheng · S. Gao · M. Chen · Y. Liu · H. Wang
Department of Microbiology and Immunology, Nantong University (Former Nantong Medical College), Nantong 226001, China

M. Fei
Institute of Medical Biotechnology, Soochow University, Suzhou 215007, China

M. Fei
Soochow University & Saier Immuno-biotech Co., Ltd., Suzhou 215123, China

J. Zhao · X. Yu
Department of Orthopaedics, Affiliated Hospital of Nantong University, Nantong 226001, China

Furthermore, colocalization of Dexras1, carboxy-terminal PSD95/DLG/ZO-1 (PDZ) ligand of nNOS (CAPON) and nNOS was observed in neurons and glial cells, supporting the existence of ternary complexes in this model. Thus, the results that the transient high expression of Dexras1 which localized in apoptotic neurons and pathological oligodendrocytes might provide new insight into the secondary response after SCT.

Keywords Spinal cord transection · Dexras1 · nNOS · Neuron · Glia · Rat

Introduction

Traumatic injury to the spinal cord is characteristically accompanied by a period of secondary cellular degeneration that occurs in injured tissue over a course of hours and days after the initial insult, and that affects both glia and neurons (Young 1993; Crowe et al. 1997; Liu et al. 1997). SCI produces a secondary protracted wave of oligodendrocyte death in degenerating white-matter tracts distant from the injury site for weeks after the initial event (Crowe et al. 1997; Liu et al. 1997; Shuman et al. 1997; Abe et al. 1999; Li et al. 1999; Casha et al. 2001), and neurons are selectively vulnerable (Grossman et al. 2001). The loss of these cells contributes to long-term neurological dysfunction involving voluntary motor control and sensory deficits below the site of injury.

Some molecules may participate in the secondary injury such as NO, which is synthesized from L-arginine by one of three isotypes of NOS (Griffith and Stuehr 1995), serving as an important neurotransmitter in CNS (Matsuyama et al. 1998; Genovese et al. 2006). NO synthesized by nNOS functions as a synaptic signaling molecule in the nervous system (Bredt and Snyder 1992) but leads to neuronal cell death when produced in excess (Beckman et al. 1990; Dawson et al. 1991; Zhang et al. 1994; Bonfoco et al. 1995; Estevez et al. 1998; Heneka et al. 1998). nNOS, a calcium (Ca^{2+})/calmodulin-dependent enzyme, was reported to be induced in many pathological processes including stroke and SCI (Miscusi 2002; Sharma et al. 2006; Bizzoco et al. 2007). One of the regulators of nNOS is *N*-methyl-D-aspartate receptor (NMDAR), an excitatory glutamate receptor consisting of NR1 and NR2 subunits which is targeted to excitatory synapses where it functions in neural plasticity (Carroll and Zukin 2002). It has been demonstrated that extracellular concentration of glutamate is markedly elevated at the site of injury and glutamate-mediated excitotoxicity contributes to progression of SCI (Yanase et al. 1995). Overstimulation of NMDAR by glutamate can lead to excessive Ca^{2+} entry, thereby activated nNOS in a Ca^{2+}/calmodulin-dependent manner (Rameau et al. 2004). Thus, the release of glutamate and the activation of nNOS clearly contribute to secondary damage following SCI.

Murine Dexras1 was first reported in 1998 by Kemppainen and Behrend (1998) as a dexamethasone-inducible gene in AtT-20 pituitary cells as well as in primary tissues including the brain, heart, and liver. The deduced protein sequence of Dexras1 showed significant homology to members of the Ras superfamily of small GTPases, with approximately 35% identity with its nearest homologs, human Rap-2b and R-Ras, over a core-conserved region. Similar to other members of the Ras superfamily, Dexras1 possesses four highly conserved motifs for GTP-binding and hydrolysis (Σ1–Σ4), an effector loop that mediates protein–protein interactions, and a membrane-targeting CAAX box which serves as a consensus site for isoprenylation. Dexras1 is distinguished from other Ras-like proteins by the presence of an extended C-terminal cationic domain (Cismowski et al. 1999).

By a yeast 2-hybrid approach, Dexras1 was identified as a binding partner for CAPON, a scaffolding protein that interacts with nNOS (Jaffrey et al. 1998). Physiological association between CAPON and Dexras1, and the existence of ternary complexes of CAPON, Dexras1, and nNOS, were confirmed in brain lysates using co-immunoprecipitation and affinity chromatography, respectively (Fang et al. 2000). Dexras1 protein was found predominantly in the cytosol with a small fraction being membraneassociated. In vitro, Dexras1 was nitrosylated by NO donors at a single putative residue, cysteine-11 (Fang et al. 2000; Jaffrey et al. 2002). Moreover, nitrosylation enhanced the guanine nucleotide exchange activity of Dexras1. In cortical neurons, NMDA stimulation resulted in a greater abundance of the GTP-loaded (and activated) form of Dexras1, an effect which was blocked by nNOS antagonists. Similarly, in $nNOS^{-/-}$ mouse brains, levels of activated Dexras1 were greatly reduced compared with wild-type controls. Our recently published article (Shen et al. 2007) demonstrated the changes in mRNA for CAPON, Dexras1, and nNOS in the sciatic nerve, dorsal root ganglia, and lumbar spinal cord of adult rat at certain time periods following sciatic axotomy. In total, the observations indicated that Dexras1 is a downstream physiological target of NMDAR-nNOS-mediated signaling. It will be important to determine which NO-dependent functions are mediated by Dexras1.

In the present study, we sought to investigate the temporal and spatial patterns of Dexras1 expression, cellular localization, association among Dexras1, CAPON, and nNOS, and probable role in cell death in SCT model. The transient high expression of Dexras1 may provide new insight into the secondary response after SCT.

Materials and Methods

Animals

A total of 72 adult Sprague Dawley rats (Department of Animal Center, Medical College of Nantong University) were used. Male rats weighing 180–220 g were kept under standard conditions and given food and water ad libitum. These included animals used for real time-PCR ($n = 24$), western blot analysis ($n = 24$), and immunofluorescence ($n = 24$). A total of 63 rats were subjected to spinal cord transection and nine were subjected to sham operation. Animals were killed at different times after injury. All surgical interventions and postoperative animal care were carried out in accordance with the Guide for the Care and Use of Laboratory Animals (National Research Council, 1996, USA), and were approved by the Chinese National Committee for the Use of Experimental Animals for Medical Purposes, Jiangsu Branch.

Surgery

A total of 63 rats received complete spinal cord transections at the T8–T10 spinal levels using procedures described previously (Bregman 1987; Bregman and McAtee 1993). Briefly, after laminectomy, the dura was opened, and the spinal cord was transected using iridectomy scissors. Vacuum suction was used to clean the most lateral recesses of the canal. The severed ends of the cord typically retracted 3–5 mm and were inspected under a surgical microscope to ensure complete transection. After the injury, the muscles and skin were closed in layers, and rats were placed in a temperature- and humidity-controlled chamber overnight. Manual bladder evacuation was performed at least thrice daily until reflex bladder emptying was established. For the sham-operated controls, the animals underwent the laminectomy without transection.

Real-time PCR

Rats were killed at 2 h, 8 h, 1 day, 3 day, 5 day, 7 day, and 14 day after transection, and sham-operated controls were killed at 2 h after the laminectomy ($n = 3$ for each group). Then, the spinal cords containing 8 mm rostral and dorsal segments were carefully removed and dipped into 1 ml TRIzol (Life technologies), respectively, stored at −80°C. Total RNA was isolated from the frozen specimens. The cDNA synthesis was carried out with RevertAid^{TM} RT Kit (Fermentas) in a 20 μl reaction volume according to the manufacturer's protocol. The cDNA was diluted 1:1 and 2 μl was used in each 20 μl PCR reaction. The procedure for real-time PCR has been described previously (Gruner et al. 2002). The amplifications were carried out in a 36-well plate in a 20 μl reaction volume containing 1× PCR buffer, 20 mM magnesium chloride, 0.2 mM deoxyNTP, 10 nmol TaqMan probe, 10 nmol of each forward (F) and reverse (R) primer, 1 U of *Taq* polymerase, and 2 μl of plasmids or cDNA samples. Oligonucleotide primer pairs and probe for Dexras1, and β_2-microglobulin (β_2-M) are shown in Table 1 in detail. Real-time PCR was performed in a Rotor-gene 3000 Detector (Corbett Research CA, USA). The thermal profiles consisted of 3 min at 94°C, followed by 40 cycles of 20 s at 94°C and 1 min at 60°C. All experiments were performed in triplicate. Copy numbers of cDNA for Dexras1 were standardized to those of β_2-M for the same sample.

Western Blot

For preparation of tissue extracts for immunoblots, spinal cords from sham, contusion at the same time as total RNA isolation ($n = 3$ for each group) were homogenized in a lysate buffer containing 1 M Tris–HCl pH 7.5, 1% Triton X-100, 1% NP-40 (nonidet p-40), 10% SDS, 0.5% sodium deoxycholate, 0.5 M EDTA, 10 μg/ml leupeptin, 10 μg/ml aprotinin, and 1 mM PMSF, and then centrifuged at 10,000*g* for 30 min to collect the supernatant. Protein concentrations were determined with a Bio-Rad protein assay (BioRad, Hercules, CA, USA). The supernatant was diluted in 2× SDS loading buffer and boiled. Proteins were separated with SDS-PAGE (5–10% gradient gels) and transferred to polyvinylidine diflouride filter (PVDF) membranes (Millipore). The membranes were blocked with 5% dried skim milk in TBST (20 mM Tris, 150 mM NaCl, and 0.05% Tween-20). After 2 h at room temperature, the filters were washed by TBST for thrice and then incubated overnight with polyclonal antibody against Dexras1 (Santa, sc-16404, 1:300) at 4°C, respectively. Finally, Rabbit-anti-Goat IgG conjugated to horseradish peroxidase (SouthernBiotech, 6020-05, 1:5,000) was added for additional 2 h and the blots were developed using enhanced chemiluminescence detection system (Pierce). After the chemiluminescence was exposed to X-ray films (Fuji Photo Film), the films were scanned using a molecular dynamics densitometer (Scion, Frederick, MD). Relative amounts of Dexras1 were quantified by optical density analysis. The level was normalized to β-actin (Sigma, A-5316, 1:1,000), a domestic loading control. In control experiments, anti-Dexras1 was blocked by pre-incubation with peptide antigen (Santa, sc-16404 P).

Table 1 Sequences of TaqMan probes and primers

Gene	Accession number	TaqMan probe (5′-3′)	Predicted size (bp)	Primers (5′-3′)
Dexras1	NM_340809	tctggcaatc atccgtttcc cg	117	F-gcggcgaagt ctaccagttg
				R-tgtctaagct gaacaccagaatga
β_2-M	NM_012512	Cacccaccgagaccgatgtatatgcttgc	134	F-gtctttctacatcctggctcaca
				R-gacggttttgggctccttca

Immunofluorescence

Rats were killed 5 day after injury, and sham-operated controls were killed at 2 h after the laminectomy. Animals were deeply anesthetized with pentobarbital (80 mg/kg, i.p.) and perfused transcardially with 500 ml of 0.9% saline, followed by 500 ml of fresh 4% paraformaldehyde. After perfusion, the spinal cord was carefully dissected out, a segment containing 8 mm rostral and caudal segments was blocked, respectively, post-fixed for an additional 2 h in the 4% paraformaldehyde. The specimens were transferred to a solution containing 30% sucrose in 0.1 M phosphate buffer (PB), pH 7.4, overnight. All sections were cut at 12 μm on a cryostat and stored at −80°C.

The sections were blocked with 10% normal goat serum containing 3% (w/v) bovine serum albumin (BSA), 0.1% Triton X-100, and 0.05% Tween-20 overnight at 4°C in order to avoid unspecific staining. Then the sections were incubated with both polyclonal antibodies specific for Dexras1 (Santa, sc-16404, 1:50), CAPON (Santa, sc-9138, 1:50), and nNOS (Sigma, N7280, 1:200), different markers as follows: monoclonal antibody for NeuN (Chemicon, MAB377, 1:600), CNP (Sigma, C5922, 1:100), GFAP (Sigma, G9269, 1:100), OX-42 (Serotec, MCA275G, 1:50), caspase-3 (Sigma, C8487, 1:200), and Tau-1 (Chemicon, MAB3420, 1:200), for 12–24 h at 4°C. After wash in PBS for thrice, each for 10 min, the secondary antibodies (TRITC-Goat-anti-Rabbit, Jackson lab, 1:100; and FITC-Goat-anti-Mouse, SBA, 1:75; TRITC-Rabbit-anti-Goat, Jackson lab, 1:100; FITC-Mouse-anti-Rabbit, SBA, 1:100) were added in dark room and incubated for 2–3 h at 4°C. To ascertain specific binding of the antibodies for the proteins, anti-Dexras1 was blocked by pre-incubation with peptide antigen (Santa, sc-16404 P) in control experiments. The images were captured by Leica fluorescence microscope (Germany).

Counting Cells

Varietal positive signals were counted in 12 μm thick transverse sections. Six sections were chosen from each animal (three animals from each group), and in each section, six specimens were obtained. The 3 mm segments adjacent to the transverse site were excluded because of nonuniformity in cord continuity and the presence of pan-necrosis. Three fields per specimen were counted at 20× magnification. The numbers of positive signals in the 18 sections were averaged.

Statistical Analysis

All values are expressed as means ± SEM. The statistical significance of differences between groups was determined by a one-way analysis of variance (ANOVA) followed by the Tukey's post hoc multiple comparison tests. $P < 0.05$ was considered significant. Each experiment consisted of at least three replicates per condition.

Results

Changes in mRNA and Protein Expression for Dexras1 After SCT

Real-time PCR was performed to investigate the temporal pattern of Dexras1 mRNA expression in SCT model. In the rostral side of the transected spinal cord, mRNA for Dexras1

slightly increased at 1 day following SCT and reached the peak at 5 day ($P < 0.05$), gradually recovering to the baseline level at 14 day (Fig. 1A, a). In the caudal side, the tendency of Dexras1 mRNA changing with time points after injury was similar to that of rostral side except for a maximum present at 3 day ($P < 0.05$) after SCT (Fig. 1A, b).

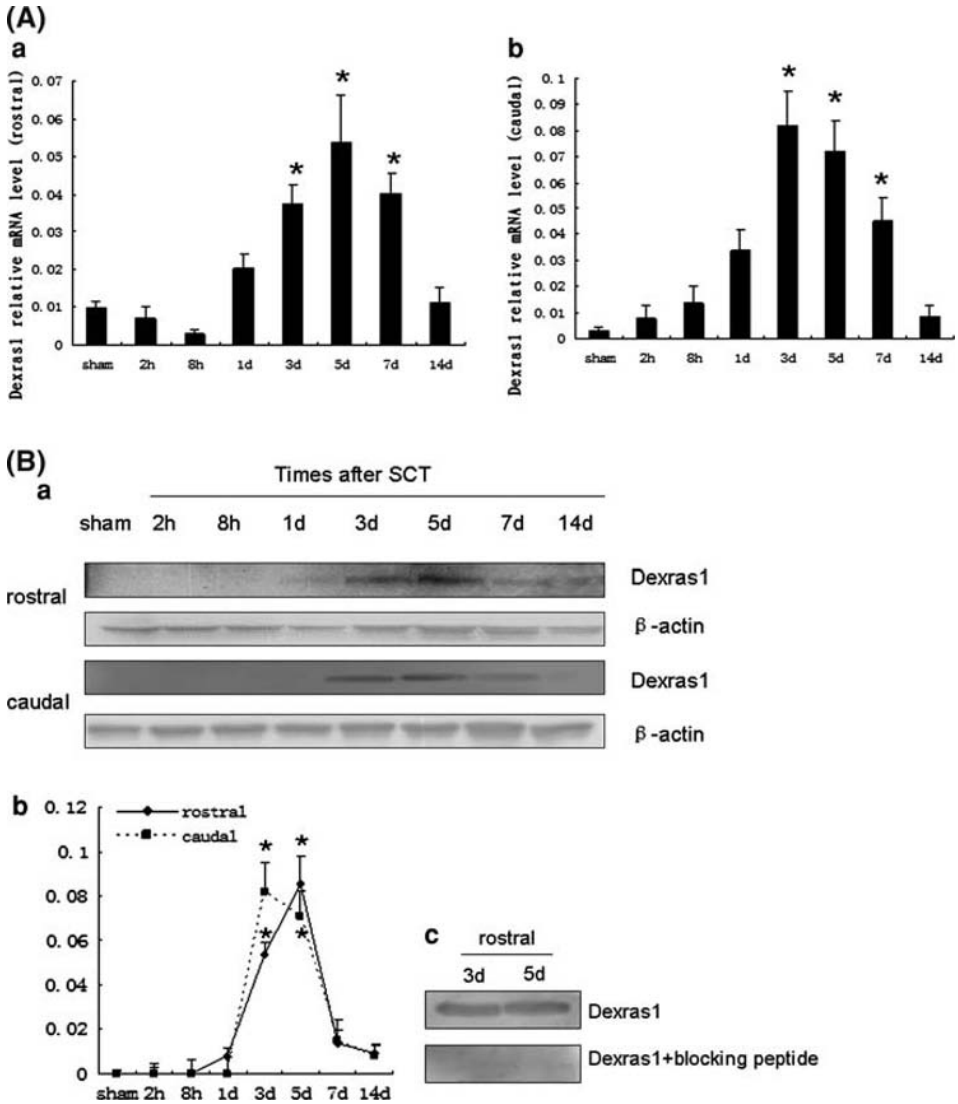

Fig. 1 Results show the change in Dexras1 at mRNA and protein level with real-time PCR and Western blot analysis in rostral and caudal spinal cord homogenate after SCT. All experiments were done at least for thrice. Statistical analyses were made with one-way ANOVA followed by Tukey's post hoc analysis. (**A**), Real-time PCR for Dexras1. The results were expressed as means ± SEM relative mRNA of the samples was normalized to that of β_2-M. In the rostral side (a) of 3, 5, and 7 day SCT groups, the levels are significantly different from that of control; In the caudal side (b), the 3 and 5 day SCT groups show the significant changes compared with control. *$P < 0.05$. (**B**), Western blot analysis for Dexras1. Representative blots (a) were showed; data were expressed (b) as means ± SEM of three samples per time point. Ratios of densities of Dexras1 to β-actin protein were compared. At 3 and 5 day after SCT the protein level is significantly different from that of control in either rostral or caudal side. *$P < 0.05$. In (c) the results are shown with and without blocking of the antibody, and the blocking peptide used as control refers to the synthetic peptide

To confirm the change in mRNA level for Dexras1 after SCT, Western blot analysis was performed to detect its protein expression. In contrast to real time-PCR analysis, Dexras1 protein expression was not detected in sham-operated controls. A band of light labeling with a molecular weight of 31 kDa appeared at 1 day after SCT in the rostral side whereas pre-incubation with peptide antigens failed to do so (Fig. 1B, c). At 3 day after transection, Dexras1 protein expression increased significantly ($P < 0.05$), and reached the peak at 5 day ($P < 0.05$), and then gradually declined from 7 to 14 day. Whereas in the caudal side, the change in Dexras1 protein was similar to the rostral side except for the highest expression present at 3 day ($P < 0.05$) that was almost identical to the mRNA level (Fig. 1B, a). Densitometric analysis revealed the change tendency of Dexras1 in both rostral and caudal side after SCT (Fig. 1B, b). These data that Dexras1 upregulated at mRNA and protein level following SCT, provided the evidence that Dexras1 might involve in pathological process following CNS injury.

Spatial Distribution of Dexras1 Immunoreactivity After SCT

Based on SCT induced transient high expression of Dexras1, immunofluorescence was performed to observe its spatial distribution. In sham-operated controls, Dexras1-IR was observed at low levels in both gray and white matters (Fig. 2A, a, c–f). At 5 day after transection, strong Dexras1-IR is significant ($P < 0.05$) compared with control based on quantitative study (Fig. 2B), extending in both rostral (data not shown) and caudal cord segments (Fig. 2A, b) and distributing in ventral horn (Fig. 2A, g), intermediate zone (Fig. 2A, h), dorsal horn (Fig. 2A, i), and white matter (Fig. 2A, j), respectively. In fact, increased Dexras1-IR was observed throughout the entire length of the cord specimen (10 mm in length). In control sections pre-incubated with peptide antigens, there was no labeling (Fig. 2A, l).

Cellular Localization of Dexras1 Immunoreactivity After SCT

With the objective to investigate the cellular localization of Dexras1 after SCT, immunofluorescence was performed at light microscopic levels. At 5 day after SCT, Dexras1 overlapped with NeuN-positive neurons in ventral horn (Fig. 3A, a–c) and other parts of gray matter (data not show), while highly expressed in the oligodendrocytes which could be appreciated in the merge of Dexras1 and CNP, the marker of oligodendrocyte in the white matter (Fig. 3A, d–f). However, in the adjacent section around the transected site, OX-42-labeled microglias were almost negative for Dexras1-IR in the white matter after SCT (Fig. 3A, g–i). Astrocytes, a subtype of glial cell intimately associated with the synapse, express all three forms of NOS (Murphy 2000). We wonder whether Dexras1 expressed in astrocytes after SCT, and the results showed Dexras1-IR presented in some astrocytes which were located in ventral horn (Fig. 3B, a–c), intermediate zone (Fig. 3B, d–f), and white matter (Fig. 3B, j–l) but not dorsal horn (Fig. 3B, g–i). Quantitative analysis of the colocalization of Dexras1 with different cellular markers summarized (Fig. 3C). These morphological observations suggested that Dexras1 might affect several neuronal and glial cell populations that contribute to pathological process after SCT.

The Colocalization of Dexras1 with Pathological Markers After SCT

Following a severe injury to the lower thoracic spinal cord in adult rats, neurons and oligodendrocytes underwent apoptosis, with a biphasic curve, probably from 3 to 7 day (Liu et al. 1997; Yong et al. 1998). Based on evidence that caspase-3 activity and expression have a

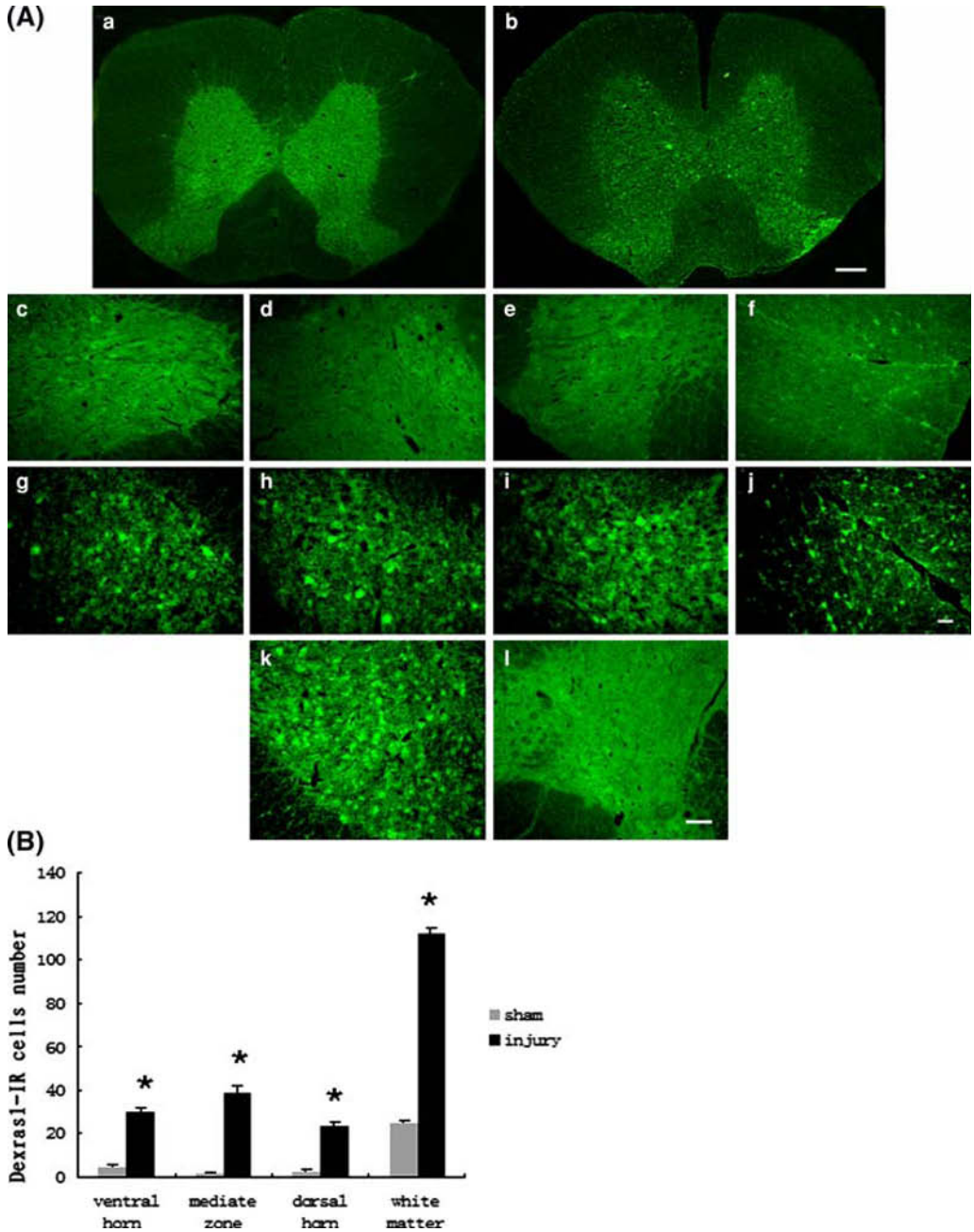

Fig. 2 Immunofluorescence results show the change and the distribution of Dexras1-IR after SCT. (**A**), The change and the distribution of Dexras1 were observed in representative photomicrographs in transverse sections of the spinal cord from sham-operated group (a) and 5 day injured group (b). Magnifield of images (c–j) for (a) and (b) showed Dexras1-IR in ventral horn (c, g), intermediate zone (d, h), dorsal horn (e, i), and white matter (f, j), respectively, in sham-operated group (c–f) and 5 day injured group (g–j). In (k, l) the results are shown with (l) and without (k) blocking of the antibody, and the blocking peptide used as control refers to the synthetic peptide. Scale bar: (a, b), 200 μm; (c–j), 50 μm; (k, l); and 100 μm. (**B**), Quantitative results for numbers of Dexras1-IR-positive cells. $*P < 0.05$ compared to sham by ANOVA followed by Tukey's post hoc analysis ($N = 18$ slices from three animals for each group, six slices per animal)

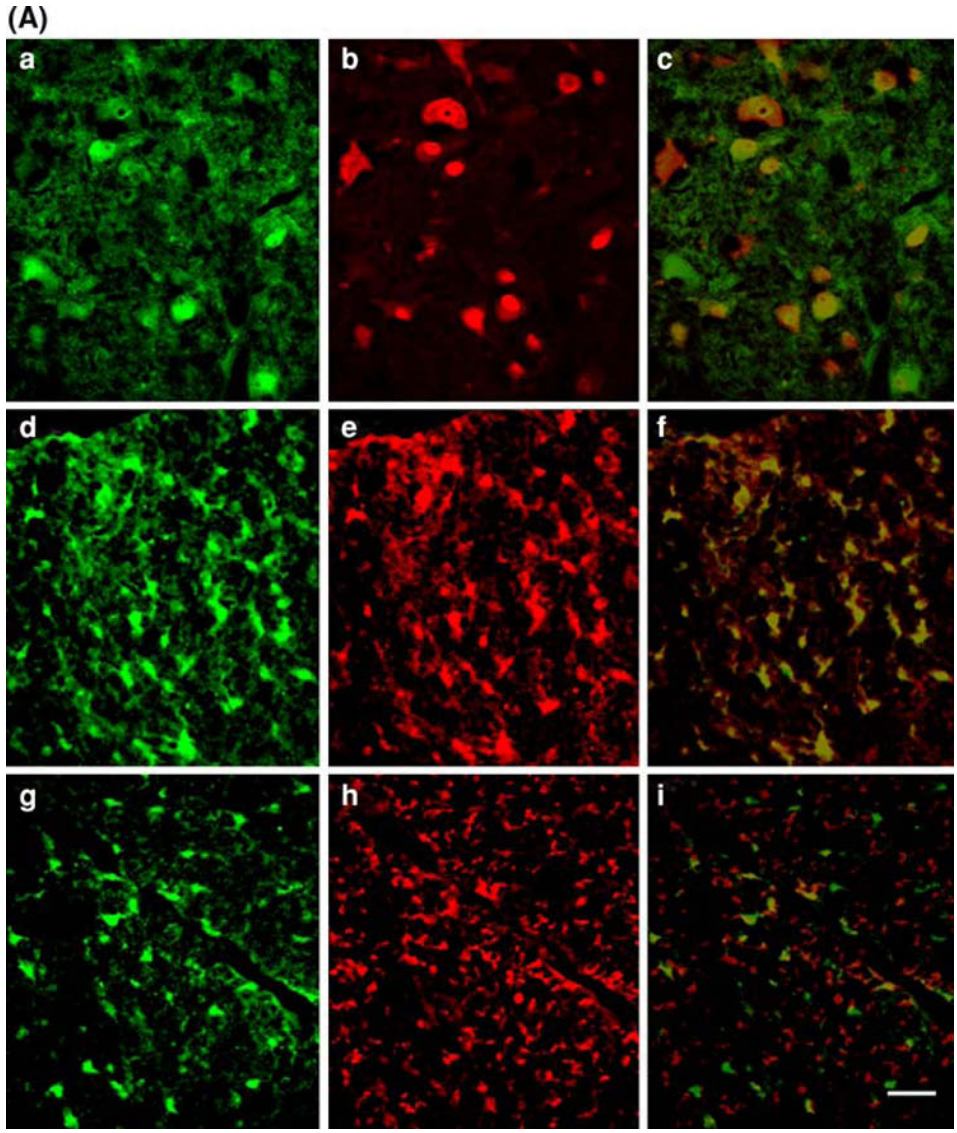

Fig. 3 Coimmunofluorescence analysis of localization of Dexras1 at 5 day after SCT. (**A**), Colocalization of Dexras1 (a, d, g) with different cellular markers: NeuN (b), CNP (e), and OX-42 (h); Panel (c, f, i) shows the merged graphs. (**B**), Colocalization of Dexras1 (a, d, g, j) with GFAP in ventral horn (b), intermediate zone (e), dorsal horn (h), and white matter (k), respectively; Panel (c, f, i, l) shows the merged graphs. Scale bar: 50 μm. (**C**), Quantitative results summarize the proportion of different cellular markers in ventral horn, intermediate zone, dorsal horn, and white matter

positive correlation with cell apoptotsis after SCI (Springer et al. 1999; Citron et al. 2000), caspase-3 is used here as an apoptotic marker to investigate whether apoptosis occurred in Dexras1-IR positive cells. First, merged images to identify the types of the dying cells in spinal cord sections demonstrated the colocalization of caspase-3 with NeuN (Fig. 4A, a–c) and CNP (Fig. 4A, d–f), suggesting delayed neuronal and oligodendrocyte death at 5 day after SCT. Second, observation of co-labeled Dexras1 with caspase-3 revealed that cell death mainly

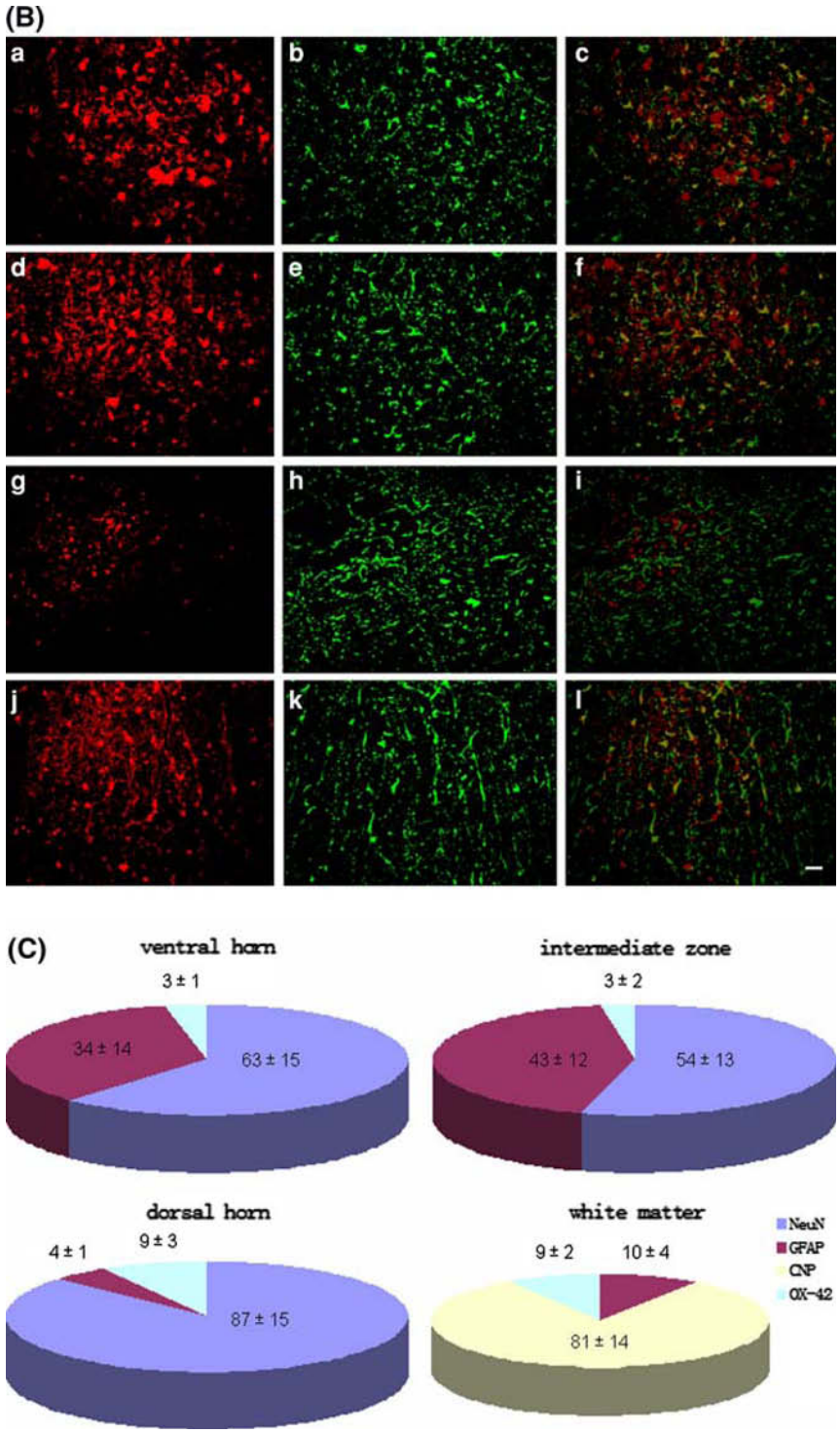

Fig. 3 continued

occurred in Dexras1-IR neurons (Fig. 4B, a–c) but scarcely in oligodendrocytes (Fig. 4B, d–f). The probable explanation is that oligodendrocytes did not experience apoptosis at this time. The results of the quantitative evaluation of the colocalization of Dexras1 with caspase-3 are summarized (Fig. 4C). Extending previous studies that oligodendrocytes injury was associated with the accumulation of microtubule-associated protein, Tau-1 (Gresle et al. 2006), the immunofluorescence labeling with Dexras1 and Tau-1 was performed. Significant content of Dexras1 was observed in many pathological oligodendrocytes, evaluated by the colocalization of Dexras1 and Tau-1 (Fig. 4B, g–i). These morphological observations suggest that the upregulation of Dexras1 in apoptotic neurons and pathological oligodendrocytes may participate in the secondary damage afer SCT.

Immunofluorescence Colocalization of Dexras1, CAPON, and nNOS After SCT

nNOS is a key enzyme for NO production that upregulated under stress such as SCI (Diaz-Ruiz et al. 2002). CAPON was originally identified as an interactor and modulator of nNOS, which is highly enriched in brain and has numerous colocalizations with nNOS (Jaffrey et al. 1998). The existence of ternary complexes of Dexras1, CAPON, and nNOS was already confirmed in brain lysates (Fang et al. 2000). To study whether Dexras1 was associated with CAPON and nNOS during the pathological process of secondary response after SCI, we performed immunnofluorescence in animals killed at 5 day after transection. The labeling was examined using Leica fluorescence microscope, and the cell type was determined by morphological and size characteristics (David et al. 2004; Faulkner et al. 2004; Martin et al. 2005). In the injured rats, expression of Dexras1 and CAPON could be localized to the same neurons in the ventral horn (data not show) and intermediate zone (Fig. 5A, a–c), but not dorsal horn (data not show). In the white matter, colocalization of Dexras1 and CAPON was observed in cells morphologically suggestive of oligodendrocytes and astrocytes (Fig. 5A, d–f). However, cells expressing either Dexras1 or CAPON were also found (Fig. 5A, d–f). Whereas, expression of Dexras1 and nNOS could be localized to the same neurons only in ventral horn (Fig. 5B, a–c) but not anywhere else in gray matter (data not show), and colocalization of them also be found in glial cells of white matter around the injured site (Fig. 5B, d–f). In sections incubated with normal goat or rabbit IgG, Dexras1-IR, CAPON-IR or nNOS-IR were not observed (data not shown). These data demonstrated that ternary complexes of Dexras1, CAPON and nNOS might have the potential role after SCT.

Discussion

In this report, temporal and spatial patterns of Dexras1 expression were investigated after SCT in adult rats. We demonstrated that CNS trauma induce Dexras1 upregulated significantly at mRNA and protein level in spinal cord homogenates. Immunofluorescence revealed that both neurons and glia showed Dexras1-IR and some pathological markers such as caspase-3 and Tau-1 partly colocalized with Dexras1. Furthermore, colocalization of Dexras1, carboxy-terminal PDZ ligand of nNOS (CAPON), and nNOS were observed in neurons and glial cells, supporting the existence of ternary complexes (Fang et al. 2000).

In the rostral side of spinal cord, changes in Dexras1 mRNA and protein expression share the same temporal pattern that is slightly increased at 1 day following SCT and reached the peak at 5 day ($P < 0.05$), gradually recovering to the baseline level at 14 day. The tendency about the caudal side is similar to that of the rostral side except for the highest expression

Fig. 4 The expression of Dexras1 in pathological cells at 5 day following SCT. (**A**), Identification of apoptotic ▶ cell types. Colocalization of caspase-3 (a, d) with NeuN (b), CNP (e). Panel (c, f) shows the merged graphs. (**B**), Colocalization of Dexras1 (a, d, g) with caspase-3 (b, e) and Tau-1 (h). Scale bar: 50 μm. (**C**), The number of Dexras1 and caspase-3 positive cells in different part of transverse sections at 5 day after SCT increased significantly compared with sham-operated. Values are expressed as mean ± SEM $^*P < 0.05$ ($n = 3$)

present at 3 day ($P < 0.05$) after SCT. The undetectable expression at Dexras1 protein level in sham-operated control and early group (2 h, 8 h) after injury is probably because of the low sensitivity of the antibody and the slight expression of Dexras1. The period from 3 to 5 day when Dexras1 was expressed highly is just included in the second wave of neuronal and glial death (Liu et al. 1997; Grossman et al. 2001) and prompt that Dexras1 might involved in cell death after SCI.

Then, the spatial distribution and cellular localization of Dexras1 by immunofluorescence showed that Dexras1-IR appeared widely in neurons located in ventral horn, intermediate zone, dorsal horn, and major oligodendrocytes, some astrocytes in white matter expressed Dexras1-IR. SCI is characteristically accompanied by a period of secondary cellular degeneration that occurs in injured tissue over a course of hours and days after the initial insult, and that affects both neurons and glial cells (Young 1993; Crowe et al. 1997; Liu et al. 1997). Recent studies examining human and rat spinal cord suggest activation of the cytochrome *c*-dependent capsase-3 apoptotic cascade in neuronal and oligodendroglial cell death after injury (Emery et al. 1998; Springer et al. 1999). Here, colocalization of Dexras1 and capsase-3 used as an apoptotic marker was observed in neuronal and several oligodendroglial cell confirmed by NeuN and CNP. Moreover, we observed the colocalization between Dexras1 and Tau-1, which has been found to be a sensitive marker for oligodendroglial injury in several studies (Rutter and Stephenson 2000; Gresle et al. 2006; Kim et al. 2006). These data further support the hypothesis that Dexras1 may participate in the circumstance of cell loss after CNS trauma.

Constitutive NOS is thought to synthesize NO in CNS neurons, and is important for intracellular signaling and neurotransmission (Bredt and snyder 1992; Saito et al. 1994). Adult motor neurons in mice deficient in nNOS- and iNOS-resisted apoptosis that is mediated by upstream NO and ONOO– genotoxicity, downstream p53, and Fas activation (Martin et al. 2005). In the current study, significantly increased expression of Dexras1 in caspase-3-IR motor neurons of ventral horn indicated that it might involved in apoptosis of motor neurons in NO-dependent manner during the process of secondary response after SCT.

In normal mice, Wallerian degeneration begins 1–2 day after axotomy (Perry et al. 1991) and demyelination was greatly prevented in mice lacking nNOS, but when demyelinating less, $nNOS^{-/-}$ mice exhibited a delay in remyelination (David et al. 2006). The morphological results that Dexras1 locaolized in the CNP-IR and Tau-1-IR oligodendrocytes in white matter provide the circumstantial evidence contributing to the demyelinatation and remyelination after SCT.

Reactive astrocytes are a prominent feature of the cellular response to SCI. Astrocytes exhibit a graded response to injury that includes changes in gene expression, hypertrophy, and process extension, and, in some cases, cell division (Eddleston and Mucke 1993; Eng and Ghirnikar 1994). Available evidence (Liuzzi and Lasek 1987; Rudge and Silver 1990; Larner et al. 1995; Finkbeiner 1995; Faulkner et al. 2004) suggested that astrocyte roles after SCI are likely to be dynamic and context-dependent, such that astrocytes may exert either pro- or anti-inflammatory functions at different locations or at different times in the response to injury and during repair. The nNOS isoform is also found in astrocytes (Kugler and Drenckhahn 1996; Cha et al. 1998). Transmitters which induce Ca^{2+} signaling in cultured murine cortical astrocytes lead to the Ca^{2+}-dependent synthesis of NO, that in turn stimulates a Ca^{2+} influx pathway that is, in part, responsible for the refilling of internal Ca^{2+} stores (Nianzhen et al.

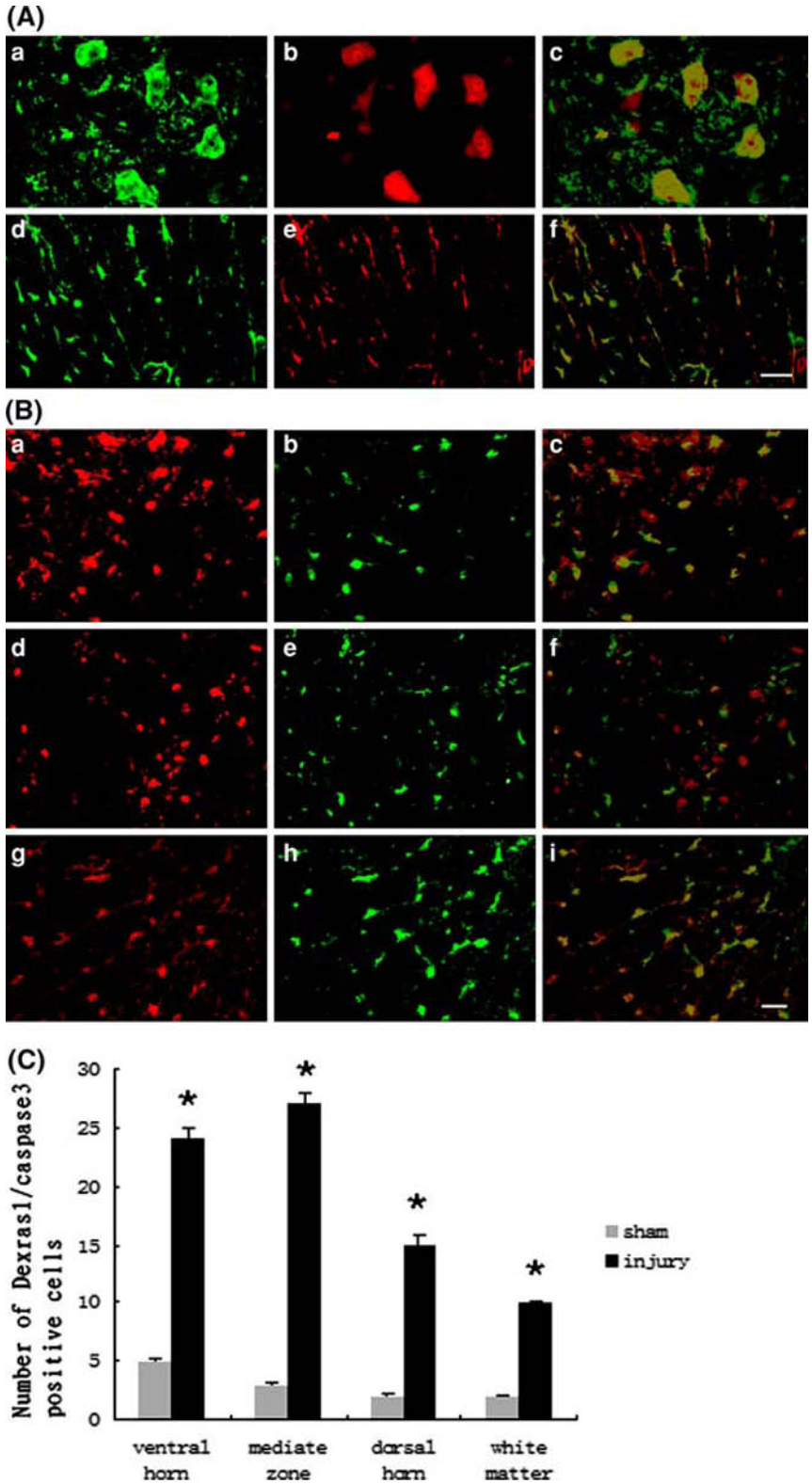
(A)
a
b
c
d
e
f
(B)
a
b
c
d
e
f
g
h
i
(C)
Number of Dexras1/caspase3 positive cells
30
25
20
15
10
5
0
*
*
*
*
ventral horn
mediate zone
dorsal horn
white matter
sham
injury

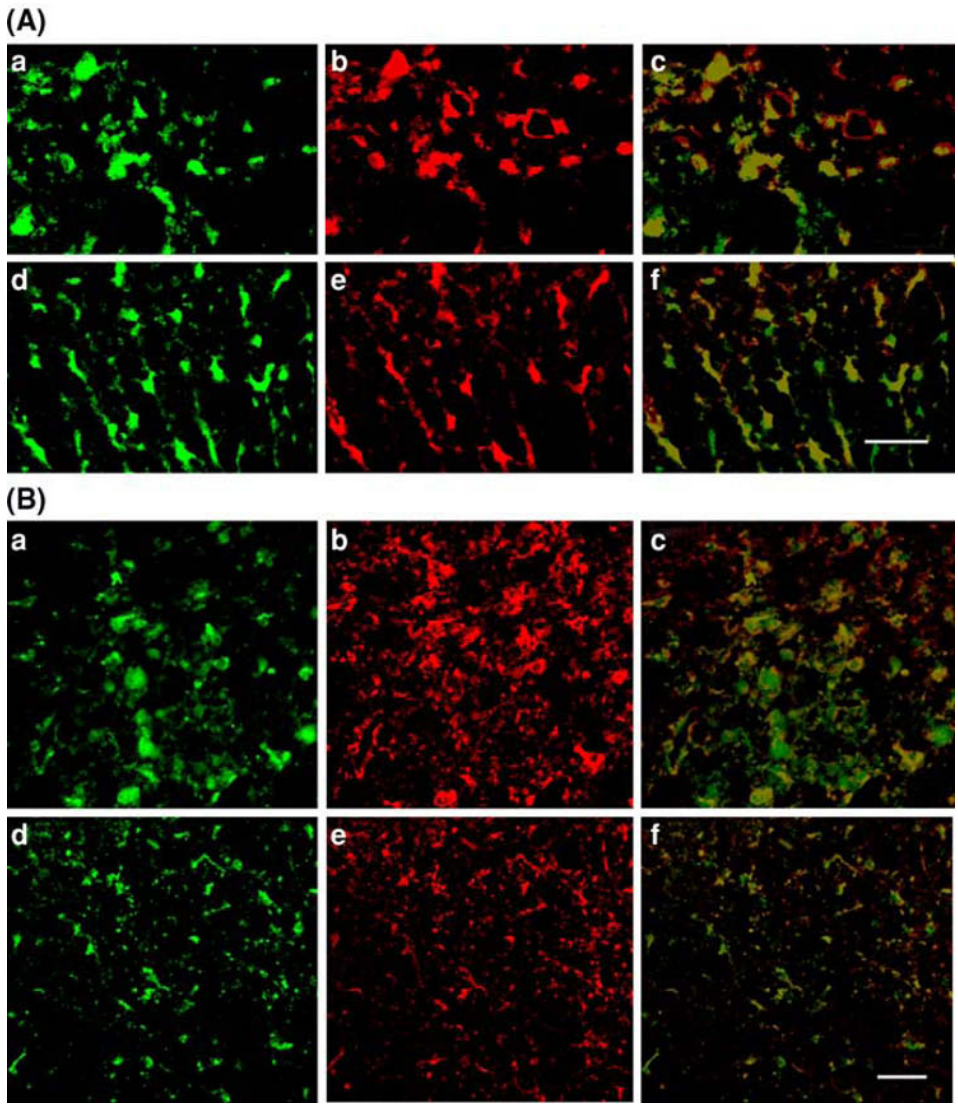

Fig. 5 Representative photomicrographs that illustrate the colocalization of Dexras1 with CAPON and nNOS in at 5 day after SCT. (**A**), colocalization of Dexras1 (a, d) with CAPON (d, e) in ventral horn (a–c) and white matter (d–f). (**B**), colocalization of Dexras1 (a, d) with nNOS (d, e) in ventral horn (a–c) and white matter (d–f). Scale bar: 50 μm

2003). Interestingly, our findings showed that reactive astrocytes distributed in ventral horn, intermediate zone, and white matter that is away from the central necrotic lesions or cavities were main resource of Dexras1, which supported the previous study (Fitch et al. 1999; Faulkner et al. 2004), providing circumstantial evidence that Dexras1 might be involved in preserving reactive astrocytes or augmenting their protective functions, which lead to novel approaches to reducing secondary tissue degeneration and improving functional outcome after damage.

Expression of Dexras1 could be observed in dorsal horn which did not show CAPON-IR at 5 day after SCT. Meanwhile, nNOS colocalized with Dexras1 in neuron only in ventral horn

but were not detected anywhere else in gray matter. The proper interpretation is that distribution of these molecule changed according to pathologic circumstances.

Glutamate is an essential mediator of excitotoxicity, which is a form of neuronal death that can occur in a variety of brain regions subsequent to ischemic insult or other neurodegenerative conditions (Arundine and Tymianski 2003). Evidence from knockout mice and other models demonstrated the contributions of NO and nNOS to glutamate-induced neuronal death (Huang et al. 1994; Dawson et al. 1996). One of the regulators of nNOS is the NMDAR, an excitatory glutamate receptor consisting of NR1 and NR2 subunits which is targeted to excitatory synapses where it functions in neural plasticity (Carroll and Zukin 2002). Cheah et al. have identified a signaling cascade in neurons whereby stimulation of NMDAR activates nNOS, leading to *S*-nitrosylation and activation of Dexras1, which, via the peripheral benzodiazepine receptor-associated protein (PAP7) and the divalent metal transporter (DMT1), physiologically induce iron uptake. As selective iron chelation prevents NMDA neurotoxicity in cortical cultures, the NMDA-NO-Dexras1-PAP7-DMT1-iron uptake signaling cascade also appears to mediate NMDA neurotoxicity (Cheah et al. 2006). Here, in SCT model, Dexras1 may participate in the secondary response, being accompanied with stimulation of NMDA receptors, activating nNOS and selective iron chelation.

Furthermore, glucocorticoids transmit molecular information to neurons and glial cells in the CNS and regulate cell function. Since Dexras1 appears to be rapidly induced by glucocorticoids in several body tissues (Kemppainen and Behrend 1998), it will be of interest to determine whether this gene participates in CNS injury through glucocorticoid action.

A number of reports have followed that refine our understanding of the role of Dexras1 in signal transduction. It has been proposed that Dexras1 might competes with G protein-coupled receptors (GPCR) to disrupt receptor-G protein signaling (Graham et al. 2002, 2004; Takesono et al. 2002), blocks activation of extracellular signal-regulated kinase (ERK 1/2) (Graham et al. 2002; Nguyen and Watts 2005), and activates the p42/p44 MAPK pathway (Cismowski et al. 2000). Dexras1 also inhibits G$\beta\gamma$-dependent heterologous sensitization of adenylyl cyclase type 1 (AC1) (Nguyen and Watts 2005) and negatively modulates AC2 signaling by interfering with PKCδ activity (Nguyen and Watts 2006). It was reported that a direct interaction between Dexras1 and the Gβ1 subunit (Hiskens et al. 2005) involves the C-terminal domain of Dexras1 (the same region that interacts with CAPON). Vaidyanathan et al. (2004) report that Dexras1 inhibit clonogenic growth of MCF-7 and A549 cells. Thus, the antiproliferative effects of Dexras1 might be associated with its role in signal transduction.

In conclusion, we demonstrated that Dexras1 is dominantly expressed in apoptic neurons and pathological oligodendrocytes after SCT. Further investigation is necessary to focus on Dexras1 in signal transduction after CNS injury and confirm the role of this gene by anti-sense oligonucleotide intrathecal injection after SCT.

Acknowledgments This work was supported by the National Natural Science Foundation of China (No. 30300099, No. 30770488), Natural Science Foundation of Jiangsu province (No. BK2003035, No. BK2006547), and "Six Talent Peak" Foundation of Jiangsu province.

References

Abe Y, Yamamoto T, Sugiyama Y, Watanabe T, Saito N, Kayama H, Kumagai T (1999) Apoptotic cells associated with Wallerian degeneration after experimental spinal cord injury: a possible mechanism of oligodendroglial death. J Neurotrauma 16:945–952

Arundine M, Tymianski M (2003) Molecular mechanisms of calcium-dependent neurodegeneration in excitotoxicity. Cell Calcium 34(4–5):325–137

Beckman JS, Beckman TW, Chen J, Marshall PA, Freeman BA (1990) Apparent hydroxyl radical production by peroxynitrite: implications for endothelial injury from nitric oxide and superoxide. Proc Natl Acad Sci USA 87:1620–1624

Bizzoco E, Vannucchi MG, Faussone-Pellegrini MS (2007) Transient ischemia increases neuronal nitric oxide synthase, argininosuccinate synthetase and argininosuccinate lyase co-expression in rat striatal neurons. Exp Neurol 204:252–259

Bonfoco E, Krainc D, Ankarcrona M, Nicotera P, Lipton SA (1995) Apoptosis and necrosis: two distinct events induced, respectively, by mild and intense insults with *N*-methyl-D-aspartate or nitric oxide/superoxide in cortical cell cultures. Proc Natl Acad Sci USA 92:7162–7166

Bredt DS, Snyder SH (1992) Nitric oxide, a novel neuronal messenger. Neuron 8:3–11

Bregman B (1987) Spinal cord transplants permit the growth of serotonergic axons across the site of neonatal spinal cord transection. Dev Brain Res 34:265–279

Bregman B, McAtee M (1993) Embryonic CNS tissue transplantation for studies of development and regeneration. Neuroprotocols 3:17–27

Carroll RC, Zukin RS (2002) NMDA-receptor trafficking and targeting: implications for synaptic transmission and plasticity. Trends Neurosci 25:571–577

Casha S, Yu WR, Fehlings MG (2001) Oligodendroglial apoptosis occurs along degenerating axons and is associated with FAS and p75 expression following spinal cord injury in rats. Neuroscience 103:203–218

Cha CI, Kim JM, Shin DH, Kim YS, Kim J, Gurney ME, Lee KW (1998) Reactive astrocytes express nitric oxide synthase in the spinal cord of transgenic mice expressing a human Cu/Zn SOD mutation. Neuroreport 9:1503–1506

Cheah JH, Kim SF, Hester LD, Clancy KW, Patterson SE, Papadopoulos V, Snyder SH (2006) NMDA receptor-nitric oxide transmission mediates neuronal iron homeostasis via the GTPase Dexras1. Neuron 51(4):431–440

Cismowski MJ, Takesono A, Ma C, Lizano JS, Xie X, Fuernkranz H (1999) Genetic screens in yeast to identify mammalian nonreceptor modulators of G-protein signaling. Nat Biotechnol 17:878–883

Cismowski MJ, Ma C, Ribas C, Xie X, Spruyt M, Lizano JS (2000) Activation of heterotrimeric G-protein signaling by a Ras-related protein. J Biol Chem 275:23421–23424

Citron BA, Arnold PM, Sebastian C, Qin F, Malladi S, Ameenuddin S, Landis ME, Festoff BW (2000) Rapid upregulation of caspase-3 in rat spinal cord after injury: mRNA, protein, and cellular localization correlate with apoptotic cell death. Exp Neurol 166:213–226

Crowe MJ, Bresnahan JC, Shuman SL, Masters JN, Beattie MS (1997) Apoptosis and delayed degeneration after spinal cord injury in rats and monkeys. Nat Med 3:73–76

David PS, Kourosh K, Jie L, Lowell TM, Christopher BM, John DS, Matt SR, Wolfram T (2004) Minocycline treatment reduces delayed oligodendrocyte death, attenuates axonal dieback, and improves functional outcome after spinal cord injury. J Neurosci 24:2182–2190

David L, Maaike T, Paula M, Manuel C, Sue F, Maria S, David OW (2006) Neuronal nitric oxide synthase plays a key role in CNS demyelination. J Neurosci 26:12672–12681

Dawson VL, Dawson TM, London ED, Bredt DS, Snyder SH (1991) Nitric oxide mediates glutamate neurotoxicity in primary cortical cultures. Proc Natl Acad Sci USA 88:6368–6371

Dawson VL, Kizushi VM, Huang PL, Snyder SH, Dawson TM (1996) Resistance to neurotoxicity in cortical cultures from neuronal nitric oxide synthase-deficient mice. J Neurosci 16:2479–2487

Diaz-Ruiz A, Ibarra A, Perez-Severiano F, Guizar-Sahagun G, Grijalva I, Rios C (2002) Constitutive and inducible nitric oxide synthase activities after spinal cord contusion in rats. Neurosci Lett 319(3):129–132

Eddleston M, Mucke L (1993) Molecular profile of reactive astrocytes: implications for their role in neurological disease. Neuroscience 54:15–36

Emery E, Aldana P, Bunge MB, Puckett W, Srinivasan A, Keane RW, Bethea J, Levi AD (1998) Apoptosis after traumatic human spinal cord injury. J Neurosurg 89:911–920

Eng LF, Ghirnikar RS (1994) GFAP and astrogliosis. Brain Pathol 4:229–237

Estevez AG, Spear N, Manuel SM, Radi R, Henderson CE, Barbeito L, Beckman JS (1998) Nitric oxide and superoxide contribute to motor neuron apoptosis induced by trophic factor deprivation. J Neurosci 18:923–931

Fang M, Jaffrey SR, Sawa A, Ye K, Luo X, Snyder SH (2000) Dexras1: a G protein specifically coupled to neuronal nitric oxide synthase via CAPON. Neuron 28:183–93

Faulkner JR, Herrmann JE, Woo MJ, Tansey KE, Doan NB, Sofroniew MV (2004) Reactive astrocytes protect tissue and preserve function after spinal cord injury. J Neurosci 24(9):2143–2155

Finkbeiner SM (1995) Modulation and control of intracellular calcium. In: Kettenmann H, Ransom BR (eds) Neuroglia. Oxford UP, New York, pp 273–288

Fitch MT, Doller C, Combs CK, Landreth GE, Silver J (1999) Cellular and molecular mechanisms of glial scarring and progressive cavitation: in vivo and in vitro analysis of inflammation-induced secondary injury after CNS rauma. J Neurosci 19:8182–8198

Genovese T, Mazzon E, Mariotto S, Menegazzi M, Cardali S, Conti A, Suzuki H, Bramanti P, Cuzzocrea S (2006) Modulation of nitric oxide homeostasis in a mouse model of spinal cord injury. J Neurosurg Spine 4(2):145–153

Graham TE, Prossnitz ER, Dorin RI (2002) Dexras1/AGS-1 inhibits signal transduction from the Gi-coupled formyl peptide receptor to Erk-1/2 MAP kinases. J Biol Chem 277:10876–10882

Graham TE, Qiao Z, Dorin RI (2004) Dexras1 inhibits adenylyl cyclase. Biochem Biophys Res Commun 316:307–12

Gresle MM, Jarrott B, Jones NM, Callaway JK (2006) Injury to axons and oligodendrocytes following endothelin-1-induced middle cerebral artery occlusion in conscious rats. Brain Res 1110:13–22

Griffith OW, Stuehr DJ (1995) Nitric oxide synthases: proper-ties and catalytic mechanism. Annu Rev Physiol 7:707–736

Grossman SD, Rosenberg LJ, Wrathall JR (2001) Temporal-spatial pattern of acute neuronal and glial loss after spinal cord contusion. Exp Neurol 168:273–282

Gruner HS, Lee G, John SW, Maeda N, Smithies O (2002) Molecular phenotyping for analyzing subtle genetic effects in mice: application to an angiotensinogen gene titration. Proc Natl Acad Sci USA 99:4602–4607

Heneka MT, Loschmann PA, Gleichmann M, Weller M, Schulz JB, Wullner U, Klockgether T (1998) Induction of nitric oxide synthase and nitric oxide-mediated apoptosis in neuronal PC12 cells after stimulation with tumor necrosis factor-a/lipopolysaccharide. J Neurochem 71:88–94

Hiskens R, Vatish M, Hill C, Davey J, Ladds G (2005) Specific in vivo binding of activator of G protein signaling 1 to the Gβ1 subunit. Biochem Biophys Res Commun 337:1038–1046

Huang Z, Huang PL, Panahian N, Dalkara T, Fishman MC, Moskowitz MA (1994) Effects of cerebral ischemia in mice deficient in neuronal nitric oxide synthase. Science 265:1883–1885

Jaffrey SR, Snowman AM, Eliasson MJ, Cohen NA, Snyder SH (1998) CAPON: a protein associated with neuronal nitric oxide synthase that regulates its interactions with PSD95. Neuron 20:115–124

Jaffrey SR, Fang M, Snyder SH (2002) Nitrosopeptide mapping: a novel methodology reveals *S*-nitrosylation of dexras1 on a single cysteine residue. Chem Biol 9:1329–1335

Kemppainen RJ, Behrend EN (1998) Dexamethasone rapidly induces a novel Ras superfamily member-related gene in AtT-20 cells. J Biol Chem 273:3129–31

Kim BG, Dai HN, McAtee M, Vicini S, Bregman BS (2006) Remodeling of synaptic structures in the motor cortex following spinal cord injury. Exp Neurol 198:401–415

Kugler P, Drenckhahn D (1996) Astrocytes and Bergmann glia as an important site of nitric oxide synthase I. Glia 16:165–173

Larner AJ, Johnson AR, Keynes RJ (1995) Regeneration in the vertebrate central nervous system: phylogeny, ontogeny, and mechanisms. Biol Rev 70:597–619

Li GL, Farooque M, Holtz A (1999) Apoptosis of oligodendrocytes occurs for long distances away from the primary injury after compression trauma to rat spinal cord. Acta Neuropathol 98:473–480

Liu XZ, Xu XM, Hu R, Du C, Zhang SX, McDonald JW, Dong HX, Wu YJ, Fan GS, Jacquin MF, Hsu CY, Choi DW (1997) Neuronal and glial apoptosis after traumatic spinal cord injury. J Neurosci 17:5395–5406

Liuzzi FJ, Lasek RJ (1987) Astrocytes block axonal regeneration in mammals by activating the physiological stop pathway. Science 237:642–645

Martin LJ, Chen K, Liu Z (2005) Adult motor neuron apoptosis is mediated by nitric oxide and Fas death receptor linked by DNA damage and p53 activation. J Neurosci 25:6449–6459

Matsuyama Y, Sato K, Kamiya M, Yano J, Iwata H, Isobe KI (1998) Nitric oxide: a possible etiologic factor in spinal cord cavitation. J Spinal Disord 11:248–252

Miscusi M (2002) The role of constitutive nitric oxide synthase in pathogenesis of secondary lesion after spinal cord injury. Preliminary results. J Neurosurg Sci 46:55–59

Murphy S (2000) Production of nitric oxide by glial cells: regulation and potential roles in the CNS. Glia 29: 1–13

Nguyen CH, Watts VJ (2005) Dexras1 blocks receptor-mediated heterologous sensitization of adenylyl cyclase 1. Biochem Biophys Res Commun 332:913–920

Nguyen CH, Watts VJ (2006) dexamethasone-induced Ras protein 1 negative regulate protein kinase C delta: implication for adenylyl cyclase 2 signaling. Mol Pharmocal 69(5):1763–1771

Nianzhen L, Jai-Yoon S, Philip GH (2003) A calcium-induced calcium influx factor, nitric oxide, modulates the refilling of calcium stores in astrocytes. J Neurosci 23(32):10302–10310

Perry VH, Brown MC, Lunn ER (1991) Very slowr etrograde and Wallerian degeneration in the CNS of C57BL/Ola mice. Eur J Neurosci 3:102–105

Rameau GA, Chiu LY, Ziff EB (2004) Bidirectional regulation of neuronal nitric-oxide synthase phosphorylation at serine 847 by the *N*-Methyl-D-aspartate receptor. J Biol Chem 279:14307–14314

Rudge JS, Silver J (1990) Inhibition of neurite growth on astroglial scars in vitro. J Neurosci 10:3594–3603

Rutter AR, Stephenson FA (2000) Coexpression of postsynaptic density-95 protein with NMDA receptors results in enhanced receptor expression together with a decreased sensitivity to L-glutamate. J Neurochem 75:2501–2510

Saito S, Kidd GJ, Trapp BD, Dawson TM, Bredt DS, Wilson DA, Traystman RJ, Snyder SH, Hanley DF (1994) Rat spinal cord neurons contain nitric oxide synthase. Neuroscience 59:447–456

Sharma HS, Wiklund L, Badgaiyan RD, Mohanty S, Alm P (2006) Intracerebral administration of neuronal nitric oxide synthase antiserum attenuates traumatic brain injury-induced blood–brain barrier permeability, brain edema formation, and sensory motor disturbances in the rat. Acta Neurochir Suppl 96:288–294

Shen A, Chen M, Niu S, Sun L, Gao S, Shi S, Li X, Lv Q, Guo Z, Cheng C (2007) Changes in mRNA for CAPON and Dexras1 in adult rat following sciatic nerve transaction. J Chem Neuroanat. doi: 10.1016/j.jchemneu.2007.07.004

Shuman SL, Bresnahan JC, Beattie MS (1997) Apoptosis of microglia and oligodendrocytes after spinal cord contusion in rats. J Neurosci Res 50:798–808

Springer JE, Azbill RD, Knapp PE (1999) Activation of the caspase-3 apoptotic cascade in traumatic spinal cord injury. Nat Med 5:943–946

Takesono A, Nowak MW, Cismowski M, Duzic E, Lanier SM (2002) Activator of G-protein signaling 1 blocks GIRK channel activation by a G-protein-coupled receptor: apparent disruption of receptor signaling complexes. J Biol Chem 277:13827–13830

Vaidyanathan G, Cismowski MJ, Wang G, Vincent TS, Brown KD, Lanier SM (2004) The Ras-related protein AGS1/RASD1 suppresses cell growth. Oncogene 23:5858–5863

Yanase M, Sakou T, Fukuda T (1995) Role of *N*-methyl-D-aspartate receptor in acute spinal cord injury. J Neurosurg 83:884–888

Yong C, Arnold PM, Zoubine MN, Citron BA, Watanabe I, Berman NE, Festoff BW (1998) Apoptosis in cellular compartments of rat spinal cord after severe contusion injury. J Neurotrauma 15:459–72

Young W (1993) Secondary injury mechanisms in acute spinal cord injury. J Emerg Med 11:13–22

Zhang J, Dawson VL, Dawson TM, Snyder SH (1994) Nitric oxide activation of poly (ADP-ribose) synthetase in neurotoxicity. Science 263:687–689